Stochastic flocculation of cohesive sediment: Analysis of floc mobility within the floc size spectrum

Federico Maggi[1]

Received 11 April 2007; revised 23 October 2007; accepted 31 October 2007; published 26 January 2008.

[1] A stochastic Lagrangian model is proposed to describe flocculation of suspended cohesive sediment flocs. This model takes into account the floc population in a parametric fashion, and predicts the time evolution of an individual floc by a sequence of stochastic aggregation and breakup events. Upon calibration on experimental data, the model was used to investigate floc mobility within the population size spectrum, bringing to light dynamical aspects not otherwise detectable with deterministic models. Our analysis showed that floc size fluctuations correlated with the population size distribution and breakup probability, and that size-dependent burst events repeated intermittently in time. Further analysis showed the effect of the floc population distribution on individual floc size transition and equilibrium, and the effect of using either a constant or variable floc capacity dimension to describe floc geometry.

Citation: Maggi, F. (2008), Stochastic flocculation of cohesive sediment: Analysis of floc mobility within the floc size spectrum, *Water Resour. Res.*, *44*, W01433, doi:10.1029/2007WR006109.

1. Introduction

[2] Flocculation dynamics of cohesive sediment flocs suspended in natural waters is of particular interest for its impact on sediment transport and deposition, and the large-scale morphodynamic evolution of coastal zones, estuaries, rivers, and water basins in general [e.g., *Dyer*, 1989; *Mehta*, 1989; *Seminara and Blondeaux*, 2001; *McAnally and Mehta*, 2001]. Among various hydrological, biophysical, and climatological factors [e.g., *Droppo et al.*, 1997; *De Boer et al.*, 2000], flocculation has a major impact on changes in floc size [e.g., *Van Leussen*, 1994], controlling floc settling velocity, and vertical fluxes of sediment. At the smallest time and length scales, the extent of time that a floc spends at a given size (floc mobility) can be crucial in determining whether that floc will remain in suspension or will deposit.

[3] Various approaches can be followed to model flocculation of cohesive sediment. One can model the rate of change of concentration of flocs with size between L and $L + \Delta L$ by using population balance equations of the type of *Smoluchowski von* [1917]. This can be done analytically only under some specific assumptions on the aggregation and breakup kernels [e.g., *Kokholm*, 1988; *Davies et al.*, 1999; *Shirvani and van Roessel*, 2001, 2002; *Leyvraz*, 2003]. More commonly, numerical solutions can be used to have a higher degree of freedom in modeling aggregation and breakup [e.g., *Rahmani et al.*, 2003; *Serra and Casamitjana*, 1998; *Flesch et al.*, 1999; *O'Melia*, 1980; *Lick and Lick*, 1988; *Lick et al.*, 1993; *Spicer et al.*, 1996]. Yet, depending on the number of classes used to discretize the floc size distribution, and the details of aggregation and breakup kinematics (i.e., collision frequency, attachment likelihood, breakup frequency and distribution functions), solution may require more or less demanding computational power, especially for parametric calibration.

[4] An approach complementary to Smoluchowski-based population balance equations is modeling the rate of change of size of an individual, "prototype" floc. A successful example of this Lagrangian modeling approach is the one proposed by *Winterwerp* [1998]

$$\frac{\mathrm{d}L}{\mathrm{d}t} = k_a c G L^{4-d_0} - k_b G^{3/2}(L - L_p)^{3-d_0} L^2, \tag{1}$$

where L_p is the primary particle size, c is the sediment mass concentration, G is the turbulence shear rate, d_0 is the three-dimensional floc capacity dimension, and k_a and k_b are aggregation and breakup parameters. Although carrying important simplifications of aggregation and breakup processes, and having no explicit solution, the advantage in using Winterwerp's model is that a steady state (or equilibrium) floc size is readily assessed analytically. For $d_0 = 2$, value averagely observed for real flocs [e.g., *Winterwerp*, 1998], the equilibrium floc size L^* is

$$L^* = L_p + \frac{k_a c}{k_b G^{1/2}}. \tag{2}$$

None of these modeling approaches, however, is capable of assessing the floc size fluctuations over time because of their deterministic nature: once the equilibrium is reached, a balance between aggregation and breakup will preserve the stable solution over time. However, if we imagine following a primary particle during its life, and compile a table of the times at which its mass increases or decreases, we will realize that the mass will change abruptly, remaining subsequently at rest for a certain time Δt until a new change will occur. The mass variation will be a

[1] Civil and Environmental Engineering, Berkeley Water Center, University of California, Berkeley, California, USA.

0043-1397/08/2007WR006109$09.00

random variable as well as the inter-event time Δt. This perspective suggests that a key feature in floc dynamics is the temporal fluctuation in floc size, calling into question the assumptions of deterministic flocculation models that invoke stable solutions, that is, with no time fluctuations. Stochastic modeling can represent an alternative framework when approaching a problem in which the substantial physics is affected by stochastic effects.

[5] The aim of this work was to explore with a mathematical model the temporal (stochastic) variability of the floc size around an equilibrium value during flocculation. Stochastic methods to solve the deterministic Smoluchowski equation have already been proposed [e.g., *Smith and Matsoukas*, 1998; *Kolodko et al.*, 1999; *Lee and Matsoukas*, 2000; *Lin et al.*, 2002; *Khelifa and Hill*, 2006b] and compared with each other [*Zhao et al.*, 2007] but none has focused on the analysis of the dynamics and mobility of an individual floc in probabilistic terms. The purpose here was to elaborate the deterministic model of equation (1) to take into account stochastic effects in particle aggregation and breakup. This approach is complementary to the ones by *Smith and Matsoukas* [1998] and *Khelifa and Hill* [2006b] as much as the Winterwerp equation is complementary to the Smoluchowski equation. Because this approach did not require solution of the entire population dynamics, fast computation and calibration on experimental data were allowed.

[6] This stochastic model was used to look into specific dynamical behaviors of flocculation that could not be otherwise detected by deterministic models. Particular attention was given to the correlation between the fluctuation distribution of $L(t)$ and the probabilities of aggregation and breakup, the intermittency patterns raising at steady state, and the impact of the population distribution on the floc size transition toward steady state. We analyzed how these features strongly depended on the particle concentration, turbulent shear rate, and the fractal model used to describe floc geometry, i.e., with either constant or variable capacity dimension.

2. Stochastic Model

2.1. Theory

[7] Prescribed that flocs can be modeled as fractal units, the number of primary particles n within a floc of size L can be written as [*Vicsek*, 1992]

$$n = (L/L_p)^{d_0}, \tag{3}$$

with d_0 the capacity (fractal) dimension of the flocs. Solving equation (3) for L and substituting it throughout equation (1), with the differential $\mathrm{d}L = (L_p n^{1/d_0-1}/d_0)\ \mathrm{d}n$, we can equivalently re-write equation (1) in terms of n as

$$\frac{\mathrm{d}n}{\mathrm{d}t} = \frac{d_0 G}{L_p^{d_0-3}}\left[c k_a n^{\frac{3}{d_0}} - G^{\frac{1}{2}} k_b n^{\frac{d_0+1}{d_0}} L_p \left(n^{\frac{1}{d_0}} - 1\right)^{3-d_0}\right]. \tag{4}$$

The factors k_a and k_b are defined as

$$k_a = k_a' \frac{1}{L_p^{3-d_0} d_0 \rho_s}, \quad k_b = k_b' \frac{1}{L_p^{3-d_0} d_0}\left(\frac{\mu}{F_y}\right)^{\frac{1}{2}}, \tag{5}$$

with k_a' and k_b' dimensionless calibration parameters, ρ_s the sediment density, μ the water dynamic viscosity, and F_y the floc strength. equation (4) can be re-written as

$$\frac{\mathrm{d}n(t)}{\mathrm{d}t} = f_a(n)n - f_b(n)n, \tag{6}$$

where $f_a(n)$ and $f_b(n)$ are the aggregation and breakup frequency functions (or rates of gain and loss) written as

$$f_a(n) = k_a' \frac{cG}{\rho_s} n^{\frac{3}{d_0}-1}, \tag{7}$$

$$f_b(n) = k_b' L_p G^{\frac{3}{2}} \left(\frac{\mu}{F_y}\right)^{\frac{1}{2}} (n^{\frac{1}{d_0}} - 1)^{3-d_0} n^{\frac{1}{d_0}}. \tag{8}$$

Given the initial value $n(0) = n_0$, the steady state solution n^* occurs when $f_a(n) = f_b(n)$ and corresponds to the number of primary particles within the equilibrium floc of size L^* as in equation (2).

[8] The Lagrangian deterministic model of equation (6) has the mathematical advantage of being written in the same form as birth-death dynamics where aggregation and breakup frequency functions $f_a(n)$ and $f_b(n)$ are the analogue of birth and death rates. Stochastic models for these types of equations and for $|\Delta n| = 1$ are well known as continuous-time discrete-state Markov-chain models. The principles of the mathematical theory of continuous-time discrete-state Markov-chain models is used within this context [e.g., *Allen*, 2003; *Allen and Allen*, 2003; *Matis and Kiffe*, 2004; *Novozhilov et al.*, 2006], but we introduce new elements to take into account that stochastic aggregation and breakup imply discrete changes $|\Delta n| \geq 1$ as in stochastic methods to solve the Smoluchowski equation [e.g., *Smith and Matsoukas*, 1998].

[9] A stochastic modeling of the time evolution of the number of primary particles n implies that n is not known with certainty but with some probability. Let the primary-particle number $n(t) \in \mathbb{N}$ be the floc state at time $t \in \mathbb{R}$, and the probability that the random variable $X(t)$ equals n at time t be defined as $p_n(t) = \mathrm{Prob}\{X(t) = n\}$. To relate the random variables $\{X(t)\}$ in time we make the following assumptions:

[10] (**i**) the system has a fixed number of primary particles $N \gg 1$;

[11] (**ii**) the probability $\mathrm{Prob}\{X(t) = n_0\}$ equals 1 at time $t = 0$, i.e., the initial state is know with certainty;

[12] (**iii**) in a suitably small time Δt only one event can occur, either aggregation or breakup;

[13] (**iv**) in a sufficiently small time Δt the probability for aggregation to occur is approximately $f_a(n)\ \Delta t$, while the probability for breakup to occur is approximately $f_b(n)\ \Delta t$;

[14] (**v**) when aggregation occurs, the probability to gain m primary particles in a single aggregation event is $p_m^a(t)$ with $1 \leq m \leq N - n$;

[15] (**vi**) when breakup occurs, the probability to lose m primary particles in a single breakup event is $p_m^b(t)$, with $1 \leq m \leq n - 1$.

[16] Based on assumptions (**iii**) to (**vi**), for a floc to have n primary particles at time $t + \Delta t$, either it is at state $n - m$ at time t and aggregation of a floc with m primary particles

occurs during Δt, or it is at state $n + m$ at time t and loss of m primary particles due to breakup occurs during Δt, or it is at state n at time t and neither mass gain nor mass loss occur during Δt. This can be formulated as the conditional probability

$$p_n(\Delta t) = \mathrm{Prob}\{\Delta X(t) = m | X(t) = n\} = \begin{cases} (n-m) f_a(n-m) p_m^a(t) \Delta t, \\ (n+m) f_b(n+m) p_m^b(t) \Delta t, \\ 1 - [(n-m) f_a(n-m) p_m^a(t) + (n+m) f_b(n+m) p_m^b(t)] \Delta t, \end{cases} \quad (9)$$

with $\Delta X(t) = X(t + \Delta t) - X(t)$. In terms of difference equations we have

$$\begin{aligned} p_n(t + \Delta t) = {} & (n-m) p_{n-m}(t) f_a(n-m) p_m^a(t) \Delta t \\ & + (n+m) p_{n+m}(t) f_b(n+m) p_m^b(t) \Delta t \\ & + p_n(t) \{1 - [(n-m) f_a(n-m) p_m^a(t) \\ & + (n+m) f_b(n+m) p_m^b(t)] \Delta t\}. \end{aligned}$$

Subtracting $p_n(t)$ from both sides and dividing by $\Delta t \to 0$ we obtain the forward Kolmogorov differential equation [*Allen*, 2003]

$$\begin{aligned} \frac{\mathrm{d}p_n(t)}{\mathrm{d}t} = {} & (n-m) p_{n-m}(t) f_a(n-m) p_m^a(t) \\ & + (n+m) p_{n+m}(t) f_b(n+m) p_m^b(t) \\ & - [(n-m) f_a(n-m) p_m^a(t) \\ & + (n+m) f_b(n+m) p_m^b(t)], \end{aligned} \quad (10)$$

which holds $\forall n \neq 1, N$. When the floc state is $n = 1$ (the primary particle) no breakup is allowed and all terms with $p_m^b(t)$ drop, whereas if $n = N$ (all particles in the system have integrated into a single floc) no further aggregation is possible, and all terms with $p_m^a(t)$ drop.

[17] Finding the probability $p_n(t)$ in equation (10) solves the stochastic modeling problem as much as finding the solution $n(t)$ in equation (6) solves the deterministic problem. However, the analytical solution to equation (10) can be difficult to find when the rates $f_a(n)$ and $f_b(n)$ are functions of the floc state n. Alternatively, a numerical approach that mirrors the assumptions made to write the forward Kolmogorov differential equation can be used. To accomplish this, we must define the inter-event time Δt, the probability $p_m^a(t)$, and the probability $p_m^b(t)$.

2.2. Inter-event Time

[18] In the case of aggregation only, it can be easily shown [e.g., *Allen*, 2003] that the inter-event time Δt_a for aggregation to occur is a continuous random variable with exponential distribution. Hence for a floc with n primary particles, the time τ to the next event has cumulative distribution

$$P(\tau \geq \Delta t_a) = e^{-f_a(n) n \Delta t_a}, \quad (11)$$

with $f_a(n)$ the rate parameter defined in equation (7). The inter-event time is calculated by substituting a random number between 0 and 1, extracted from a uniform distribution, to $P(\tau \geq \Delta t_a)$ in equation (11), which is next solved for Δt_a. As f_a is a monotonically increasing function of n and c, the time Δt_a will decrease with n and c increasing. Similarly, a negative exponential distribution function can be written for the inter-event time Δt_b for breakup to occur by exchanging $f_a(n)$ with $f_b(n)$, and Δt_a with Δt_b in equation (11). Following assumption **(iii)** that exclusively one process between aggregation and breakup occurs, we extract the aggregation and breakup inter-event times Δt_a and Δt_b from their cumulative distributions, and determine Δt by taking

$$\Delta t = \min\{\Delta t_a, \Delta t_b\}. \quad (12)$$

This procedure also serves to determine which of the two events is to happen, that is, if $\Delta t_a < \Delta t_b$ aggregation will occur, vice versa otherwise.

2.3. Stochastic Aggregation

[19] For $\Delta t_a < \Delta t_b$, a gain of m primary particles will occur with a probability $p_m^a(t)$ that we can define as

$$p_m^a(t) = p_m(t) \alpha_{n,m}(t), \quad (13)$$

where $p_m(t)$ is the probability for a floc with n primary particles to collide with a floc with m primary particles, and $\alpha_{n,m}(t)$ is the probability for these to attach.

[20] The probability $p_m(t)$ is, in essence, the size distribution of the floc population at time t, and is a model input that can be provided in various ways, including the distribution measured in real experiments, or a polynomial expression as in *Khelifa and Hill* [2006b]. In this modeling approach we will give preference to an analytical description of $p_m(t)$ to conveniently take into account the effect of time and shear rate. From experimental optical recording carried out in settling column tests [*Maggi*, 2007], the steady state floc primary-particle distribution can be described with a lognormal probability distribution function

$$p_m(\infty) = \frac{1}{[m(L)]\sqrt{2\pi\sigma^2(\infty)}} e^{-\frac{1}{2}\frac{\{\ln[m(L)] - \mu(\infty)\}^2}{\sigma^2(\infty)}}, \quad (14)$$

where $m(L)$ is the number of primary particles in a floc of size L. The distribution parameters for the steady state floc populations

$$\sigma^2(\infty) = \log[1 + s_m^2/\overline{m}^2], \quad (15)$$

$$\mu(\infty) = \log[\overline{m}] - \sigma^2(\infty)/2, \quad (16)$$

are computed from the average number of primary-particle in a floc, $\overline{m}$, and variance, s_m^2, obtained form the same experimental data (Table 1). Finally, p_m is normalized such that $\Sigma p_m \Delta m = 1$. Equation (14) reproduces reasonably well empirically acquired floc distributions (Figure 1). Although a first approximation, the use of lognormal distributions has been shown in earlier works [e.g., *Lambert et al.*, 1981; *McCave*, 1984; *Burban et al.*, 1989] to agree well with real distributions. Equation (14) is therefore used as a starting point to introduce in this stochastic model a floc distribution in a mathematically simple way, and to allow numerical

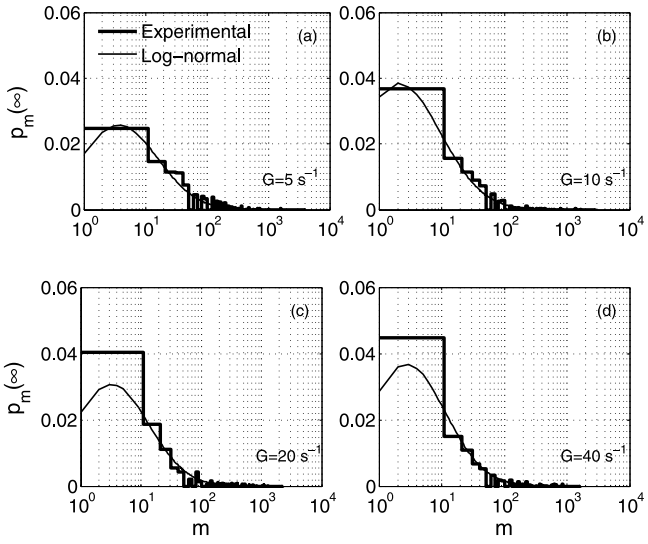

Figure 1. Steady state floc primary-particle distributions measured in settling column tests at various turbulence shear rates G, and for mass concentration $c = 0.5$ kg m^{-3}. Values of m were determined via equation (3) by measuring the size L of individual flocs and estimating their capacity dimension d_0 from optical recordings [*Maggi and Winterwerp*, 2004]. The sediment used was kaolinite with $L_p \approx 5$ μm and density $\rho_s = 2650$ kg m^{-3}.

computation with ease compared to other techniques, e.g., by solution of the Smoluchowski equation.

[21] In order to take into account the effect of time on p_m during the transition toward steady state we introduce the timescale T. For $0 < t < T$, we can write σ^2 and μ of equation (14) as functions of t as follows

$$\mu(t) = \mu(0) + [\mu(\infty) - \mu(0)]\frac{t}{T}, \tag{17}$$

$$\sigma^2(t) = \sigma^2(0) + [\sigma^2(\infty) - \sigma^2(0)]\frac{t}{T}. \tag{18}$$

The parameters $\mu(0)$ and $\sigma^2(0)$ describe the initial lognormal distribution $p_m(0)$, while $\mu(\infty)$ and $\sigma^2(\infty)$ describe the steady state $p_m(\infty)$ for $t > T$.

[22] The probability of effective attachment $\alpha_{n,m}(t)$ between two interacting flocs in equation (13) depends on their hydrodynamic interaction. This interaction can be expressed in terms of floc size using the formulation by *Pruppacher and Klett* [1978] later extended to include hydrodynamic effects due to the flocs porosity via their capacity dimensions [*Maggi*, 2007]

$$\alpha_{n,m}(t) = \frac{9}{d_3(L(n))d_3(L(m))}\frac{R^2}{2[1+R]^2}, \tag{19}$$

with $R = \frac{\min\{L(n),L(m)\}}{\max\{L(n),L(m)\}}$ and $0 < \alpha_{n,m} < 1$.

[23] The product $p_m(t)\alpha_{n,m}(t)$ is normalized such that the cumulative $\sum p_m(t)\alpha_{n,m}(t) \cdot \Delta m$ equals 1; next, the cumulative is used to determine the gain m following aggregation and the new floc state $n(t + \Delta t) = n(t) + m$.

[24] Finally, because of assumption (**i**), we assume that any change in floc state $n(t) \rightarrow n(t + \Delta t)$ will not affect the population distribution $p_m(t)$.

2.4. Stochastic Breakup

[25] Breakup occurs in our model when $\Delta t_a \geq \Delta t_b$. Determining the loss m during fragmentation is not a straightforward task as it presupposes some knowledge of the number of fragments and their mass distribution while, at present, there is no general consensus on this aspect or direct, visual evidence such as imaging recording.

[26] Many works have been devoted to numerical analysis of the effect of various breakup kinematics on the floc size distribution. Breakup into binary fragments with equal mass was one of the first hypothesis, and was later extended to ternary breakup (e.g., one floc with half mass and two flocs with one fourth of the mass of the originating floc [*Spicer and Pratsinis*, 1996; *Flesch et al.*, 1999]). Multiple fragmentation with binomially distributed mass was shown to give better results for the time evolution of the floc size distribution [e.g., *Serra and Casamitjana*, 1998; *Mietta et al.*, 2005], but it is not supported by direct evidence, and had the disadvantage of making the computation very onerous when solving the Smoluchowsi equation. Binary fragmentation into flocs with mass extracted from a uniform distribution was recently shown by *Khelifa and Hill* [2006b] to achieve an apparent success while retaining model simplicity. However, binary breakup with either equal mass or mass extracted from a uniform distribution may combine various breakup mechanisms with no chance to distinguish surface erosion and fracture from one another [e.g., *Mietta et al.*, 2005; *Khelifa and Hill*, 2006b]. To address this, an interesting insight came from 2D and 3D mechanistic (rheologic) breakup models by *Higashitani and Iimura* [1998] and *Higashitani et al.* [2001], which took into account various attractive forces among the particles, and the drag force from the fluid. Their results suggested that fragmentation produces a spectrum of daughter flocs distributed with a power law (i.e., many small fragments, and relatively few large fragments). They also suggested that a floc with high fractal dimension disintegrates into a smaller number of flocs with high fractal dimension, while a floc with low fractal dimension produces a larger number of flocs with a broader distribution.

[27] To best approximate these observations, this model describes breakup as a binary process that satisfies assump-

Table 1. Statistical Parameters of the Floc Distributions of Figure 1 Expressed in Terms of Primary-Particle Number and Floc Size[a]

G		[s^{-1}]	5	10	20	40
Average	$\overline{m}$		89.1	73.1	72.2	58.6
% Std. deviation	s_m		241.4	228.5	191.2	152.1
Median	m_{50}		30.8	22.2	25.5	21.1
μ			3.4	3.1	3.2	3.0
σ^2			2.1	2.3	2.1	2.0
Average	$\overline{L}$	[μm]	60.6	54.9	54.5	49.1
% Std. deviation	s_L	[μm]	39.4	38.3	35.1	31.2
Median	L_{50}	[μm]	30.8	22.3	25.5	21.1

[a]These quantities are related to each other via equation (3) for a value of capacity dimension $d_0 = 2$.

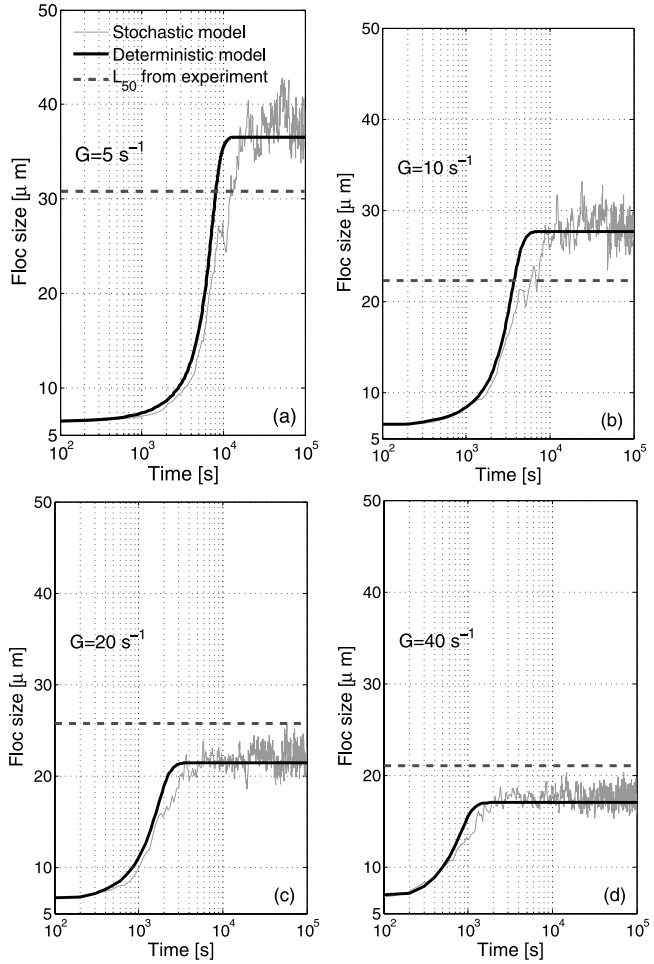

Figure 2. Deterministic and stochastic modeling results compared to experimental L_{50} for sediment mass concentration $c = 0.5$ kg m^{-3} and various shear rates G. The curve corresponding to stochastic model is the average of 100 realizations.

tion (**iii**). The mass loss m is modeled here with a power law probability distribution

$$p_m^b = m^{-\frac{d_0}{3-d_0}\beta}, \tag{20}$$

where m is in the range $1 \leq m \leq n-1$ with $n \geq 2$, and β is a calibration parameter. p_m^b is normalized such that $\sum p_m^b \Delta m = 1$. Breakup is described in equation (20) in terms of capacity dimension d_0 in a manner consistent with surface erosion of single primary particles or detachment of small fragments when $d_0 \approx 3$, and fragmentation into floc with broader distribution when $d_0 < 3$. In addition, multiple fragmentation can be interpreted as a sequence of binary breakup events that extend over a larger time extent.

[28] Finally, m is randomly extracted from the cumulative probability $\sum p_m^b \Delta m$, so that $n(t + \Delta t) = n(t) - m$.

3. Results

3.1. Model Calibration

[29] The deterministic and stochastic models of equation (6) and equation (10) share the aggregation and breakup parameters k_a' and k_b'. Calibration of k_a' and k_b' was performed by using the deterministic model with the experimental median floc size L_{50} of the four data sets of Figure 1. For these experiments we used sediment with primary-particle size $L_p = 5$ μm, density $\rho_s = 2650$ kg/m^3, concentration $c = 0.5$ kg/m^3, estimate floc strength $F_y = 3 \cdot 10^{-11}$ N, and floc capacity dimension $d_0 = 2$. Calibration resulted in $k_a' = 0.30$ and $k_b' = 1.5 \cdot 10^{-6}$. Determination of k_a' and k_b' also allowed for the use of the deterministic model to calculate with a tolerance criterium the timescale T required in equations (17) and (18) of the stochastic model. Next, the lognormal floc distributions $p_m(t)$ of Figure 1 were used in the stochastic model, and the breakup exponent $\beta = -0.41$ of equation (20) was suitably calibrated in a way that the average value of $L(t)$ computed with the stochastic model approximated $L^* \simeq L_{50}$ at steady state.

[30] Initial conditions $n(0) = 1$ and $p_{m=1}(0) = 1$ were applied to all simulations by using $\mu(0)$ and $\sigma(0)^2$ sufficiently smaller than 1 so that the lognormal distribution collapsed into a Dirac distribution with $p_{m=1}(0) = 1$.

[31] Simulations comparing experimental observations of the four data sets and predictions of L_{50} from deterministic and stochastic modeling are represented in Figure 2. Although the median size predicted by the two models overestimated the experimental one for low G-values (Figures 2a and 2b), and underestimates it for high G-values (Figures 2c and 2d), the difference was small and in the order of magnitude of 5 μm. Floc growth, as already observed by *Lick and Lick* [1988], *Burban et al.* [1989], *Oles* [1992], *Winterwerp* [1998], and *Khelifa and Hill* [2006b], showed a first exponential growth followed by a gentle approach to equilibrium.

[32] An attempt to replicate Burban's observations was performed by using the parameters calibrated here. However, the results (omitted here) did not match well with his measurements. This observation can be ascribed to differences in the test material. The sediment collected in site by Burban was made of a mixture of many minerals (e.g., calcite, chlorite, dolomite, illite, kaolinite, montmorillonite, potassium feldspar, and quartz), while the experiments used to calibrate the deterministic and stochastic models presented here were carried out with only kaolinite minerals. This test suggested that the parameters calibrated here could not be considered of general validity, but rather, sediment specific.

3.2. Effect of Mass Concentration and Turbulence Shear Rate

[33] Changes in c and G impact the shape of the steady state floc distribution $p_m(\infty)$ [e.g., *Dyer*, 1989] and, in turn, the median floc size. To integrate their effect into $p_m(t)$, we elaborated further on the parameter $\mu(\infty)$ as follows. The median $m_{50} = e^{\mu(\infty)}$ of the steady state lognormal floc distribution $p_m(\infty)$ can be written in terms of L_{50} as $m_{50} = (L_{50}/L_p)^{d_0} = e^{\mu(\infty)}$ by using the fractal scaling in equation (3). Next, having at our disposal the solution of $L^* \simeq L_{50}$ from the deterministic model for any c and G in equation (2), we can obtain $\mu(\infty)$ as

$$\mu(\infty) = d_0 \ln\left[1 + \frac{k_a c}{k_b L_p G^{1/2}}\right]. \tag{21}$$

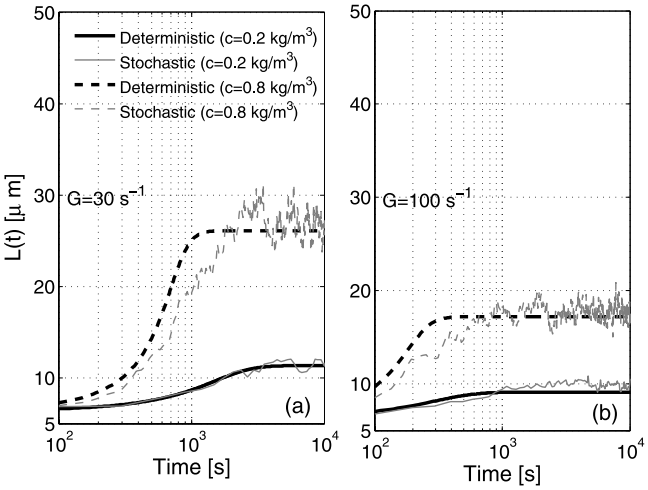

Figure 3. Comparison between stochastic and deterministic modeling for various values of mass concentration c and shear rate G.

Substituting equation (21) into equation (17) we obtain a mass concentration- and shear rate-dependent parameter $\mu(t)$ for the population distribution $p_m(t)$ for use in the stochastic model. The value $\sigma^2(\infty) = 2.2$ from Table 1 was instead kept invariant.

[34] The stochastic and deterministic models matched well for various combinations of c and G (Figure 3). Predictions of L_{50} qualitatively agreed with prior theoretical and experimental works [*Dyer*, 1989], i.e., decreasing for G increasing and increasing for c increasing within the range 0−10 kg/m^3. The model is expected to depart from real observations for c exceeding this range, as further increases in mass concentration were suggested to lead to lower L_{50} [*Dyer*, 1989].

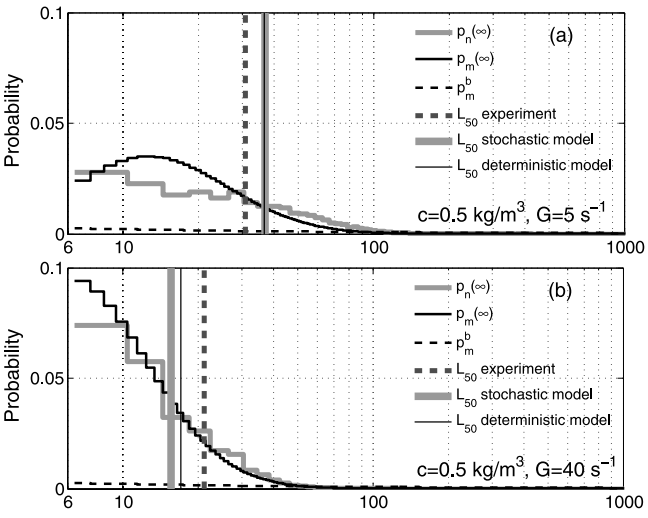

Figure 4. Comparison between the probabilities $p_n(\infty)$, $p_m(\infty)$, and p_m^b calculated, respectively, from equations (10), (14), and (20) for two combinations of mass concentration c and shear rate G.

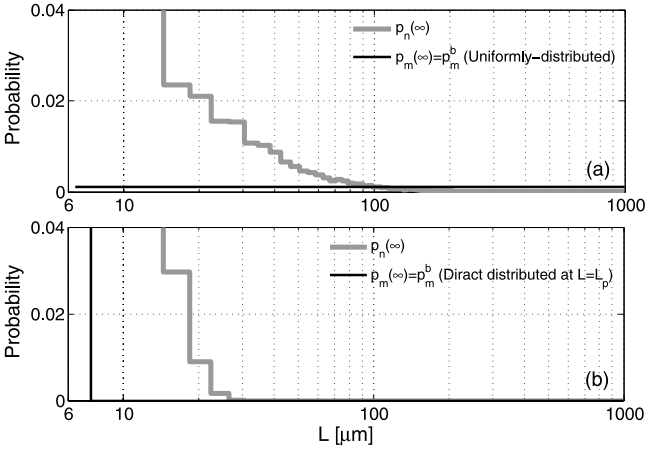

Figure 5. Comparison between probability distribution $p_n(\infty)$ from equation (10), floc population distribution $p_m(\infty)$, and breakup probability distribution p_m^b for, (*a*), $p_m(\infty) = p_m^b$ uniform, and (*b*), $p_m(\infty) = p_m^b$ Dirac-distributed. These simulations refer to mass concentration $c = 0.5$ kg m^{-3} and shear rate $G = 50$ s^{-1}.

3.3. Correlation Between $p_n(t)$, $p_m(t)$ and p_m^b

[35] The mobility of a floc of size $L(t)$ within the population size spectrum is related to the population and breakup probability distributions $p_m(t)$ and p_m^b. Their combined effect determines the fluctuations of $L(t)$ around its average $L^* \simeq L_{50}$, and, consequently, the shape of $p_n(t)$.

[36] Limiting this analysis to the steady state, the fluctuations $p_n(t)$ of $L(t)$ and the population distribution $p_m(t)$ are highly correlated for various values of G, while the correlation between $p_n(t)$ and p_m^b is low (Figure 4). The strong correlation of $p_n(t)$ with $p_m(t)$ was found to hold for a wide range of c as well (data not shown).

[37] The correlation of $p_n(t)$ with $p_m(t)$ and p_m^b drops drastically if we consider a suspension that is uniformly distributed and binary breakup is modeled as in *Khelifa and Hill* [2006b] by uniformly distributed fragments (Figure 5a). A similar drop in correlation is obtained if the suspension is Dirac-distributed at the primary particle size and breakup consists of erosion of primary particles (Figure 5b).

[38] These results show that when stochastic processes of aggregation and breakup are either white noises with $|\Delta n| \geq 1$ or colored noises with $|\Delta n| = 1$ there still remains a characteristic distribution of the fluctuations of $L(t)$ at steady state, hence, a characteristic shape of $p_n(\infty)$.

3.4. Intermittency

[39] Three single realizations (i.e., no repetition and averaging is applied) of the time evolution of $L(t)$ respectively computed for increasing sediment mass concentration c and turbulent shear rate G are represented in Figures 6a–6c. The floc size $L(t)$ passed through bursts characterized by alternation of high and low rates of aggregation or breakup. During a burst, $L(t)$ varied largely in time. Visual comparison of panels (*a*) through (*c*) suggests that, in general, the burst frequency sensibly increased with c and G, while it shortened in duration. Re-scaling the time with $(cG)^{-1}$ qualitatively showed that burst frequency was nearly independent from c and G, suggesting a more general timescale-

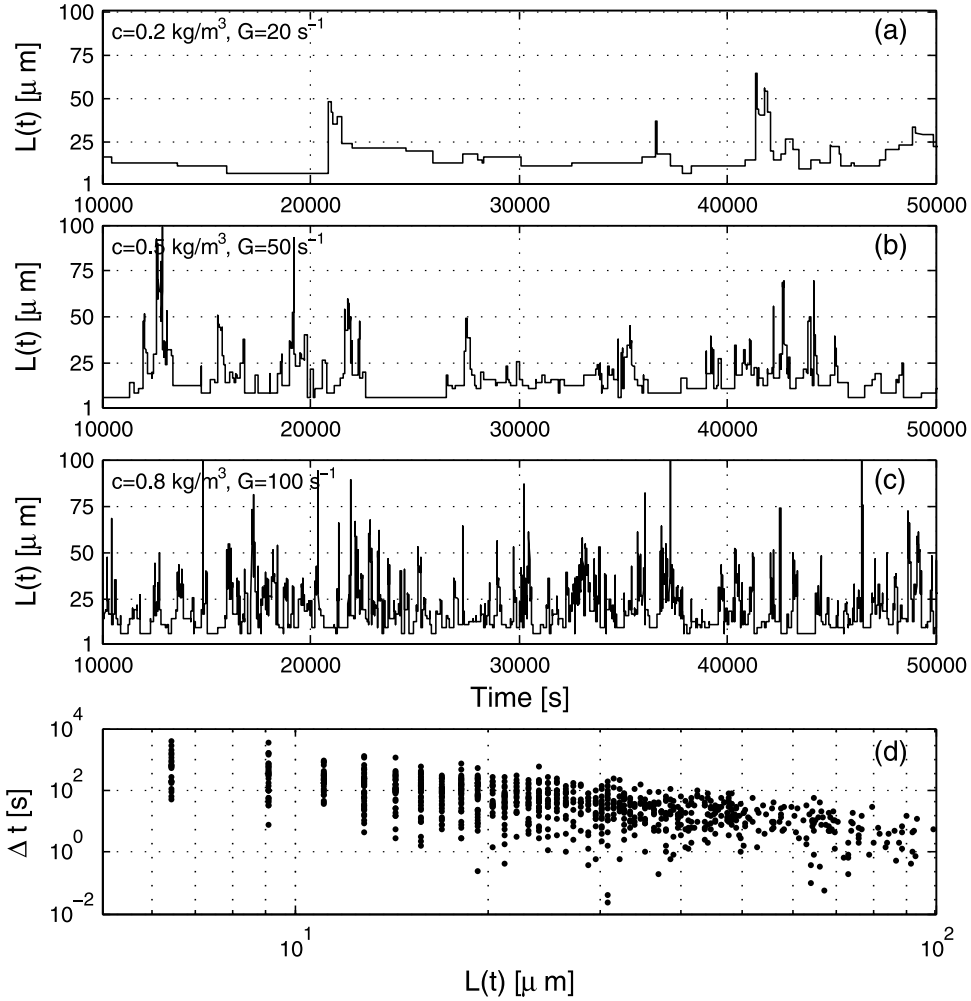

Figure 6. (a)–(c) single-realization stochastic modeling of the time evolution of the floc size $L(t)$ for three combinations of mass concentration c and shear rate G. (d) relation between $L(t)$ and the right-adjacent inter-event time Δt for $G = 20\ s^{-1}$ and $c = 0.2\ kg\ m^{-3}$.

invariant burst behavior during dynamical equilibrium (data not shown).

[40] This behavior in floc dynamics was rather unexpected, and, together with the results in section 3.3, gave a very different picture of floc mobility compared to deterministic models, in which steady state floc size, once reached, remains invariant. Emergence of more or less rapid bursts with highly variable L values can be explained as a result of the combined effects of the rates $f_a(n)$ and $f_b(n)$ and probabilities $p_m^a(t)$ and p_m^b of stochastic aggregation and breakup. For small L, $f_a(n)$ and $f_b(n)$ determine large Δt, retaining L constant for relatively long time extents. For large L, instead, $f_a(n)$ and $f_b(n)$ determine small inter-event times Δt. $L(t)$ and the right-adjacent inter-event time Δt are therefore negatively correlated (Figure 6d), with Δt spanning more than four orders of magnitude for floc sizes ranging less than two orders. Variability in $L(t)$, instead, is regulated by the probabilities $p_m^a(t)$ and p_m^b to gain or lose m primary particles following stochastic aggregation and breakup.

[41] Correlation time lag (computed from the autocorrelogram) for the fluctuating component of $L(t)$ of the three time sequences in Figures 6*a*–6*c* was found to increase first, and decrease for higher c and G (data not shown). A Fourier analysis also showed that there was no specific frequency associated with the bursts, and that the power spectral density could be described with a power law with constant slope comprised between -2 and -1 (data not shown). No further interpretation was attempted, but we believe that more mathematical analysis in this direction, supported by experimental data, could lead to additional clarifying aspects of floc dynamics and mobility within the size spectrum.

3.5. Transition Toward Steady State

[42] The floc size $L(t)$ predicted by deterministic and stochastic modeling evolved with similar shape and flocculation timescale T for $p_m(t)$ evolving from the initial Dirac probability $p_{m=1}(0) = 1$ toward the lognormal probability $p_m(\infty)$ (e.g., Figures 2 and 3).

[43] By relaxing the prescribed initial condition, two cases emerge that are worthy of study to understand the effect of $p_m(t)$ on $L(t)$ and T: the first is when a floc grows within a steady state population ($p_m(t) = p_m(\infty)\ \forall t$), while the second is when a floc grows within a Dirac-distributed population ($p_m(t) = p_{m=1}(0) = 1\ \forall t$), case typical of

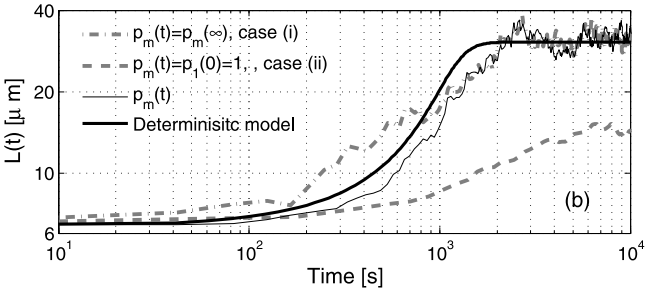

Figure 7. Time evolution of the floc size $L(t)$ computed with permanently steady state ($p_m(t) = p_m(\infty)$ − case *i*) and permanently Dirac-distributed ($p_m(t) = p_{m=1}(0)$ − case *ii*) floc populations. These are compared with $L(t)$ computed with evolving $p_m(t)$ and with the deterministic model. Mass concentration $c = 0.8$ kg/m^3 and turbulence shear rate $G = 20$ s^{-1} were used.

diffusion-limited aggregation processes [*Meakin*, 1991]. In both cases, $p_m(t)$ should feed back some dynamical patterns to $L(t)$ not capturable by the deterministic model neither in terms of equilibrium size nor in terms of timescales, as the latter does not account for the population probability distribution p_m. To reveal these aspects with the stochastic model, the following two initial conditions were used; (*i*) for $\mu(t) \equiv \mu(\infty)$ and $\sigma^2(t) \equiv \sigma^2(\infty)$ in equations (17) and (18) the probability $p_m(t)$ is permanently at steady state $p_m(\infty)$; (*ii*) for $\mu(t) \equiv \mu(0)$ and $\sigma^2(t) \equiv \sigma^2(0)$ the probability $p_m(t)$ remains equal to the initial distribution $p_{m=1}(0) = 1$.

[44] When a floc evolved within a steady state population, the stochastic and deterministic models predicted the same equilibrium (median) floc size, which reached steady state within identical timescale T (Figure 7). Condition (*i*) (i.e., $p_m(t) = p_m(\infty)$) represented the case for the floc to potentially grow most rapidly, and produced the upper boundary for the time evolution of $L(t)$ during transition toward steady state. Conversely, when a floc evolved within a Dirac-distributed population centered at the primary particle size, the flocculation timescale for the individual floc became larger than that of the deterministic model, and the steady state floc size never reached the value foretold by the deterministic model. This can be explained by the trade-off between aggregation with only primary particles and breakup into power law distributed fragments, the balance of which turns into an averagely smaller floc. Condition (*ii*) (i.e., $p_{m=1}(t) = 1$) produced the lower boundary for the time evolution of an individual floc. As a result, the transition of $L(t)$ within an evolving population (solid thin line in Figure 7) was always comprised between the limit cases depicted by the dashed and dotted lines of the stochastic model. It is possible to find analogue boundaries to the symmetric problem, that is, for the initial value $L(0)$ larger that the equilibrium one (data not shown).

3.6. Constant Fractal Dimension

[45] The deterministic and stochastic models responded differently to changes in capacity dimensions d_0 (Figures 8a, 8b). In the deterministic model, T increased slightly with d_0 increasing, while the equilibrium floc size decreased. In the stochastic model, instead, we observed the opposite behavior: both T and the equilibrium floc size increased with d_0 increasing.

[46] The behavior of the deterministic model can be explained in terms of aggregation and breakup rates; in fact, while aggregation scales with $f_a(n) \propto n^{(3-d_0)/d_0}$, breakup scales with $f_b(n) \propto n^{(4-d_0)/d_0}$, the balance being in favor of breakup for increasing d_0. This scaling holds for the stochastic model, too. However, in this case, the time to reach steady state and the equilibrium floc size depends also on the probabilities $\alpha_{n,m}$ and p_m^b, which are not taken into account in the deterministic model. For d_0 increasing, $\alpha_{n,m}$ decreases, and so does the average rate of aggregation. However, an increasing d_0 causes breakup to occur more likely as erosion of small particles rather than fracture. This behavior would yield an overall balance in favor of aggregation, hence producing larger flocs. By letting d_0 vary over the range 1.7–2.3, the equilibrium floc size increased proportionally to d_0 and the sediment mass concentration, behavior that repeated for various combinations of c and

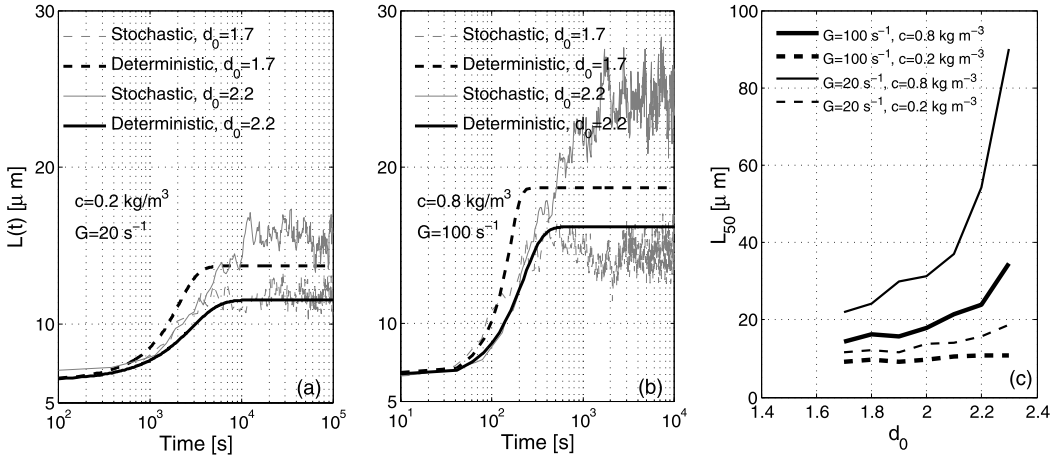

Figure 8. (a)-(b) comparisons between the time evolution of the floc size $L(t)$ computed with the stochastic and deterministic models for capacity dimensions $d_0 = 1.7$, 2.2, and for two combinations of mass concentration c and shear rate G. (c) relation between the median floc size computed with the stochastic model for increasing d_0 and four combinations of c and G.

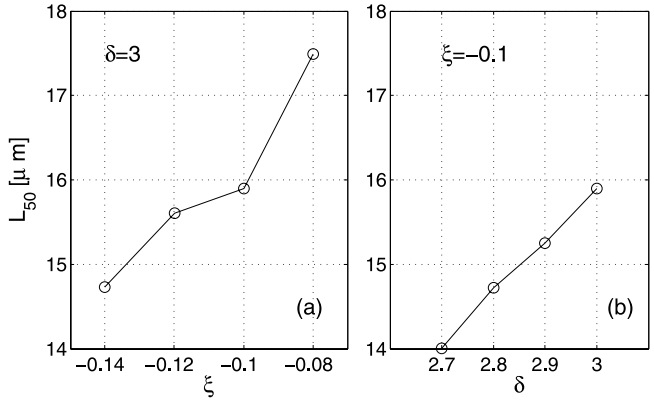

Figure 9. (a) median floc size computed with the stochastic model for various values of ξ of equation (22). (b) median floc size computed for various values of primary-particle capacity dimension δ. Simulations were run with c = 0.2 kg m^{-3} and $G = 20$ s^{-1}.

G (Figure 8c). High values of G produced small flocs regardless of d_0.

[47] Although the author is unaware of specific experimental data sets to be used for comparison, it appears physically sound to expect larger equilibrium flocs for higher capacity dimension. In fact, a more compact particle network and a higher number of contacts per particle would make flocs stronger against breakup in turbulently agitated environments, while lower capacity dimensions would result in fragile, smaller flocs.

3.7. Variable Fractal Dimension

[48] Recent experimental and modeling investigations have shown that d_0 may not be constant during floc growth but, rather, changing with the floc size at constant hydraulic and sedimentological conditions, the behavior successfully described with a power law function of L as [*Maggi*, 2005, 2007; *Khelifa and Hill*, 2006a]

$$d_0(L) = \delta\left(\frac{L}{L_p}\right)^{\xi}, \tag{22}$$

where δ is the primary particle capacity dimension and ξ is the rate of change of d_0 with L. If we use equation (22) to describe variations in capacity dimension, the rates $f_a(n)$ and $f_b(n)$, and aggregation and breakup probabilities $p_m^a(t)$ and p_m^b will be affected. To explore this effect, we implemented equation (22) in both deterministic and stochastic models, and a second calibration was performed (data not shown) resulting in $k_a' = 0.4$, $k_b' = 1.87 \cdot 10^{-4}$, $\beta = 0.08$, and with $\delta = 3$ and $\xi = -0.1$ taken from *Maggi* [2005]. Though not shown here, variable capacity dimension improved predictions of the experimental median size L_{50} in both deterministic and stochastic models with respect to using a constant capacity dimension. This improvement is consistent with the one stemming from application of equation (22) in deterministic [*Maggi et al.*, 2007] and stochastic [*Khelifa and Hill*, 2006b] Smoluchowski-based population balance equations to model the floc size distribution.

[49] The primary-particle capacity dimension δ and the exponent ξ can vary with the crystal structure of the minerals and the sediment mixture. An increasing ξ caused the average equilibrium floc size L_e to increase (Figure 9a). Similarly, an increasing values of ξ produced larger median floc sizes (Figure 9b). Increasing values of c caused higher values of L_e while increasing values of G produced lower L_e as already observed in Figure 3 (data not shown).

4. Conclusions

[50] The stochastic model for flocculation of cohesive sediment presented here has been addressed to analyze the dynamical behavior of the floc size around an average value, calibrated on the modal floc size observed in real suspensions.

[51] Model results have highlighted interesting aspects of floc mobility within the population size spectrum: (*i*) the probability distribution of the fluctuations of $L(t)$ largely correlated with the population floc size distribution, and minimally depended on the breakup probability distribution; (*ii*) floc dynamics were strongly marked by burst events repeating in time rather irregularly; (*iii*) flocculation timescales and floc size transition toward steady state were limited by upper and lower bounds determined by the initial conditions $p_m(0)$; (*iv*) the equilibrium floc size and flocculation timescales were largely impacted by various, but constant, values of floc capacity dimension; (*v*) a variable floc capacity dimension improved predictions of the median floc size and gave a higher degree of freedom in taking into account the mineralogic characteristics of the sediment at the primary particle scale.

[52] **Acknowledgments.** The author is particularly grateful to Paul Hill for having addressed important comments to the modeling approach described in the manuscript, and to two anonymous reviewers. The author is also grateful to James Hunt and Carolyn Remick for having provided a general overview of the presentation, results and analyses of this work.

References

Allen, L. J. S. (2003), *An introduction to stochastic processes with application to biology*, Pearson Education, INC., Upper Saddle River, New Jersey 07458.

Allen, L. J. S., and E. J. Allen (2003), A comparison of three different stochastic population models with regard to persistence time, *Theor. Population Biol.*, *64*, 439–449.

Burban, P.-Y., W. Lick, and J. Lick (1989), The flocculation of fine-grained sediments in estuarine waters, *J. Geophys. Res.*, *94*(C6), 8323–8330.

Davies, S. C., J. R. King, and J. A. D. Wattis (1999), The Smoluchowski coagulation equations with continuous injection, *J. Phys. A; Math Gen*, *32*, 7745–7763.

De Boer, D. H., M. Stone, and L. M. J. Lévesque (2000), Fractal dimensions of individual flocs and floc population in streams, *Hydrol. Processes*, *14*, 653–667.

Droppo, I. G., G. G. Leppard, D. T. Flanning, and S. N. Liss (1997), The freshwater floc: A functional relationship of water and organic and inorganic floc constituents affecting suspended sediment properties, *Water Air Soil Pollut.*, *99*, 43–54.

Dyer, K. R. (1989), Sediment processes in estuaries: Future research requirements, *J. Geophys. Res.*, *94*(c10), 327–332, No. 14.

Flesch, J. C., P. T. Spicer, and S. E. Pratsinis (1999), Laminar and turbulent shear-induced flocculation of fractal aggregates, *Am. Inst. Chem. Eng.*, *45*(5), 1114–1124.

Higashitani, K., and K. Iimura (1998), Two-dimensional simulation of the breakup process of aggregation in shear and elongational flows, *J. Colloid Interface Sci.*, *204*, 320–327.

Higashitani, K., K. Iimura, and H. Sanda (2001), Simulation of deformation and breakup of large aggregates in flows of viscous fluids, *Chem. Eng. Sci.*, *56*, 2927–2938.

Khelifa, A., and P. S. Hill (2006a), Models for effective density and settling velocity of flocs, *J. Hydraul. Res.*, *44*(3), 390–401.

Khelifa, A., and P. S. Hill (2006b), Kinematic assessment of floc formation using a Monte Carlo model, *J. Hydraul. Res.*, *44*(4), 548–559.
Kokholm, N. J. (1988), On Smoluchowski's coagulation equation, *J. Phys. A: Math. Gen.*, *21*, 839–842.
Kolodko, A., K. Sabelfeld, and W. Wagner (1999), A stochastic method for solving Smoluchowski's coagulation equation, *Math. Comput. Simulations*, *49*(1–2), 57–79.
Lambert, C. E., C. Jehanno, N. Silverberg, J. C. Bruncottan, and R. Chesselet (1981), Log-normal distributions of suspended particles in the open ocean, *J. Mar. Res.*, *39*(1), 77–98.
Lee, K., and T. Matsoukas (2000), Simultaneous coagulation and break-up using constant-N Monte Carlo, *Powder Technol.*, *110*, 82–89.
Leyvraz, F. (2003), Scaling theory and exactly solved models in the kinetics of irreversible aggregation, *Phys. Rep.*, *383*, 95–212.
Lick, W., and J. Lick (1988), On the aggregation and disaggregation of fine-grained sediments, *J. Great Lakes Res.*, *14*(4), 514–523.
Lick, W., H. Huang, and R. Jepsen (1993), Flocculation of fine-grained sediments due to differential settling, *J. Geophys. Res.*, *98*((C6)−10), 279–288.
Lin, Y., K. Lee, and T. Matsoukas (2002), Solution of the population balance equation using constant-number Monte Carlo, *Chem. Eng. Sci.*, *57*, 2241–2252.
Maggi, F. (2005), *Flocculation dynamics of cohesive sediments*. PhD thesis, Delft, Universitiy of Technology.
Maggi, F. (2007), Variable fractal dimension: A major control for floc structure and flocculation kinematics of suspended cohesive sediment, *J. Geophys. Res.*, *112*, C07012, doi:10.1029/2006JC003951.
Maggi, F., and J. C. Winterwerp (2004), Method for computing the three-dimensional capacity dimension from two-dimensional projections of fractal aggregates, *Phys. Rev.*, *E 69*, 011405.
Maggi, F., F. Mietta, and J. C. Winterwerp (2007), Effect of variable fractal dimension on the floc size distribution of suspended cohesive sediment, *J. Hydrol.*, *343*(1–2), 43–55.
Matis, J. H., and T. R. Kiffe (2004), On stochastic logistic population growth models with immigration and multiple births, *Theor. Population Biol.*, *65*, 89–104.
McAnally, W. H., and A. J. Mehta (2001), Coastal and estuarine fine sediment processes. Proceedings in Marine Science, 3. Elsevier, Amsterdam, The Netherlands.
McCave, I. N. (1984), Size spectra and aggregation of suspended particles in the deep ocean, *Deep Sea Res.*, *31*(4), 329–352.
Meakin, P. (1991), Fractals aggregates in geophysics, *Rev. Geophys.*, *29*.
Mehta, A. J. (1989), On estuarine cohesive sediment suspension behavior, *J. Geophys. Res.*, *94*(c10), 14303–14314.
Mietta, F., F. Maggi, and J. C. Winterwerp (2005), Sensitivity to breakup functions in a population balance equation for cohesive sediments, *Proceeding of the 8th INTERCOH Conference*, Saga, Japan. In press.
Novozhilov, A. S., G. P. Karev, and E. V. Koonin (2006), Biological applications of the theory of birth-and-death processes, *Briefings in Bioinformatics*, *7*(1), 70–85.
Oles, V. (1992), Shear-induced aggregation and breakup of polystyrene latex particles, *J. Colloid Interface Sci.*, *154*, 351–358.
O'Melia, C. (1980), Aquasols: The behaviour of small particles in aquatic systems, *ES&T*, *14*(9), 1052–1060.
Pruppacher, H. R., and J. D. Klett (1978), *The microphysics of clouds and precipitation*. Riedel, Dordrecht.
Rahmani, N., J. Masliyah, and T. Dabros (2003), Characterization of asphaltenes aggregation and fragmentation in a shear field, *AIChE J.*, *49*, 1645–1650.
Serra, T., and X. Casamitjana (1998), Modelling the aggregation and break-up of fractal aggregates in shear flow, *Appl. Sci. Res.*, *59*, 255–268.
Shirvani, M., and H. J. van Roessel (2001), Some results on the coagulation equation, *Nonlinear Analysis: Theory, Methods, and Applications*, *43*, 563–573.
Shirvani, M., and H. J. van Roessel (2002), Existence and uniqueness of solutions of Smoluchowski's coagulation equation with source terms, *Q. Appl. Math.*, *60*(1), 183–194.
Seminara, G., and P. Blondeaux (2001), River, Coastal and Estuarine Morphodynamics, Springer-Verlag, Berlin, Germany.
Smith, M., and T. Matsoukas (1998), Constant-number Monte Carlo simulation of population balances, *Chem. Eng. Sci.*, *53*(9), 1777–1786.
Smoluchowski von, M. (1917), Versuch einer Mathematischen Theorie der Koagulations-kinetik Kolloid Losungen, *Zeitschrift fur Physikalische Chemie*, *92*, 129–168, (Leipzig, in German).
Spicer, P. T., and S. E. Pratsinis (1996), Universal steady state particle size distribution, *AIChE J.*, *42*(6), 1612–1618.
Spicer, P. T., S. E. Pratsinis, M. D. Trennepohl, and G. H. M. Meesters (1996), Coagulation and fragmentation: The variation of shear rate and time lag for attainment of steady state, *Ind. Eng. Chem. Res.*, *35*, 3074–3080.
Van Leussen, W. (1994), *Estuarine Macroflocs*, Ph.D. Thesis, University of Utrecht, The Netherlands.
Vicsek, T. (1992), *Fractal growth phenomena*, World Scientific, Singapore.
Winterwerp, J. C. (1998), A simple model for turbulence induced flocculation of cohesive sediment, *J. Hydraul. Eng. Res.*, *36*(3), 309–326.
Zhao, H., A. Maisels, T. Matsoukas, and C. Zheng (2007), Analysis of four Monte Carlo methods for the solution of population balances in dispersed systems, *Powder Technol.*, *173*, 38–50.

F. Maggi, Civil and Environmental Engineering, Berkeley Water Center, University of California, 413 O'Brien Hall, Berkeley, CA 94720-1710, USA. (fmaggi@berkeley.edu)